A Hamiltonian system for interacting Benjamin–Feir resonances

2005 J. Phys. A: Math. Gen. 38 5381

(http://iopscience.iop.org/0305-4470/38/24/001)

INSTITUTE OF PHYSICS PUBLISHING JOURNAL OF PHYSICS A: MATHEMATICAL AND GENERAL

J. Phys. A: Math. Gen. **38** (2005) 5381–5403 doi:10.1088/0305-4470/38/24/001

A Hamiltonian system for interacting Benjamin–Feir resonances

T Benzekri[1,2], C Chandre[1], R Lima[1] and M Vittot[1]

[1] Centre de Physique Théorique[3], CNRS Luminy, Case 907, F-13288 Marseille Cedex 9, France
[2] Université des Sciences et de Technologie H B, BP 32, El Alia, Bab Ezzouar, Alger, Algeria

E-mail: benzekri@cpt.univ-mrs.fr, chandre@cpt.univ-mrs.fr, lima@cpt.univ-mrs.fr and vittot@cpt.univ-mrs.fr

Received 17 January 2005, in final form 4 April 2005
Published 1 June 2005
Online at stacks.iop.org/JPhysA/38/5381

Abstract

In this paper, we present a model describing the time evolution of two-dimensional surface waves in gravity and infinite depth. The model of six interacting modes derives from the normal form of the system describing the dynamics of surface waves and is governed by a Hamiltonian system of equations of cubic order in the amplitudes of the waves. We derive a Hamiltonian system with two degrees of freedom from this Hamiltonian using conserved quantities. The interactions are those of two coupled Benjamin–Feir resonances. The temporal evolution of the amplitude of the different modes is described according to the parameters of the system. In particular, we study the energy exchange produced by the modulations of the amplitudes of the modes. The evolution of the modes reveals a chaotic dynamics.

PACS number: 05.45.−a

1. Introduction

In 1967, Benjamin and Feir [1] studied the linear stability of periodic solutions of permanent form for gravity surface waves in infinite depth. They showed that wave trains are unstable to modulation perturbation, i.e., that instabilities occur due to the interaction of the carrier wave and two wave perturbations. This kind of instability was first found by Lighthill [2] and confirmed theoretically and experimentally by Benjamin and Feir. This result was also confirmed by Zakharov [3] using a Hamiltonian formalism for the surface wave problem. This instability was interpreted in terms of resonance conditions between the carrier wave and the two side bands. Later in 1977, Lake *et al* [4] observed in wave tank experiments the first modulation and demodulation of the recurrence Fermi–Pasta–Ulam phenomenon [5].

[3] Unité Mixte de Recherche (UMR 6207) du CNRS, et des universités Aix-Marseille I, Aix-Marseille II et du Sud Toulon-Var. Laboratoire affilié à la FRUMAM (FR 2291).

Many works using the Hamiltonian formalism which was first derived by Zakharov have been carried out to understand the time evolution of the resonant interaction phenomenon [6–8]. We refer in particular, for three dimensions, to Shemer and Stiassnie [9], Stiassnie and Shemer [10], Shrira *et al* [11] and Badulin *et al* [12]. In two dimensions, we refer to Benzekri *et al* [13], Caponi *et al* [14] who use a seven mode model in order to show chaotic behaviour. In order to study the long-time evolution of surface waves, Zufiria [15] derived from the Zakharov water wave equations a simple model of three interacting modes (equation (10) in [15]) which leads to chaotic behaviour. However, this model is not invariant by time reversal symmetry.

Other works using the Hamiltonian formalism in fluid interfaces were carried out in [16, 17].

In order to give a qualitative description of the spatio-temporal evolution of the dynamical system described by a Hamiltonian water wave system, we propose in our work a simple model using all the symmetries of the initial equations of surface waves. In particular, we use the time reversal symmetry to derive a system of Hamilton's equations describing the dynamics of Benjamin–Feir resonant waves. This symmetry plays an important role in the study of the system. The evolution of the complex amplitudes of the modes is governed by a cubic dynamical system of equations. The system is then a set of six ordinary differential equations. We show the existence of invariants that reduce this system to two degrees of freedom.

We use a geometrical approach to understand the energy exchange mechanism among the modes of the wave. For some initial conditions, we find that the Benjamin–Feir resonance leads to a continual periodic energy transfer from one component of the wave to the others. We also find by numerical simulations an irregular transfer of energy among the modes of the wave. The energy transfer of this kind is related to the existence of chaos in our system.

This paper is organized as follows: in section 2, we describe the model which is an approximation of the Zakharov Hamiltonian water wave system developed by Krazitskii [18]. In this model, the interactions require the coexistence of two resonating four-wave interactions. The Hamiltonian of this model written in normal form is of order four in the amplitudes of the wave.

The system has six degrees of freedom, then having six equations for the complex amplitudes. We find four integrals of motion thanks to the Manley–Rowe relations. Therefore, we reduce the model to a Hamiltonian system with two degrees of freedom.

The knowledge of these invariants allows us to subdivide the phase space into different regions and determine analytical solutions such as travelling and standing waves. In particular, we analyse how the system behaves starting from different initial conditions. Section 3 is devoted to the study of the dynamics of the system with only one resonance. The study of the chaotic dynamics with the two interacting resonances is done in section 4.

2. The model

In an inviscid and incompressible fluid approximation, the equations of the two-dimensional gravity waves on the surface of deep water read as follows [3]:

$$\Delta\varphi(x, y, t) = 0, \qquad \text{for} \quad -\infty < y < \eta(x, t), \tag{1}$$

$$g\eta(x, t) + \frac{\partial\varphi}{\partial t}(x, y, t) + \frac{1}{2}|\nabla\varphi(x, y, t)|^2 = 0, \qquad \text{for} \quad y = \eta(x, t), \tag{2}$$

$$\frac{\partial\eta}{\partial t}(x, t) + \frac{\partial\varphi}{\partial x}(x, y, t)\frac{\partial\eta}{\partial x}(x, t) - \frac{\partial\varphi}{\partial y}(x, y, t) = 0, \qquad \text{for} \quad y = \eta(x, t), \tag{3}$$

$$\lim_{y\to-\infty} \nabla\varphi(x, y, t) = 0, \tag{4}$$

where g is the strength of the gravity and the unknown variables are the surface shape of the wave η and the velocity potential φ. Zakharov [3] showed that these equations can be expressed in a Hamiltonian form

$$\frac{\mathrm{d}a_k}{\mathrm{d}t} = -\mathrm{i}\frac{\partial H}{\partial a_k^*}, \qquad \text{for} \quad k \in \mathbb{R}, \tag{5}$$

where the complex amplitudes a_k are linear combinations of the Fourier coefficients of $\eta(x,t)$ and of the free surface velocity potential $\psi(x,t)$ defined by

$$\psi(x,t) = \varphi(x, \eta(x,t), t).$$

If we restrict ourselves to the spatially periodic waves then $k \in \mathbb{Z}$. More precisely, if we define the Fourier expansion of the wave

$$\eta(x,t) = \frac{1}{2\pi}\sum_{k=-\infty}^{+\infty} \eta_k \, \mathrm{e}^{\mathrm{i}kx},$$

the relation between the coefficients η_k and the complex symplectic coordinates a_k is

$$\eta_k(t) = \frac{g^{-1/4}}{\sqrt{2}}|k|^{1/4}(a_k + a_{-k}^*).$$

The Hamiltonian is given by the total energy of the system when expressed as a function of the a_k (see [18]).

Our model is obtained by truncating the general (infinite-dimensional) Hamiltonian derived by Zakharov in the form stated by Krazitszkii [18] up to order four and retaining a minimal set of modes in order to describe a Benjamin–Feir instability for gravity surface waves in infinite depth.

In order to preserve time-reversal symmetry, this minimal number of complex modes is six, $\pm k_1, \pm k_2, \pm k_3$ that leads to a set of two coupled resonances verifying

$$k_1 + k_2 = 2k_3 \qquad \text{and} \qquad \omega_{k_1} + \omega_{k_2} = 2\omega_{k_3}, \tag{6}$$

together with the dispersion relation

$$\omega_k = \sqrt{g|k|}, \qquad \text{for} \quad k = \pm k_1, \pm k_2, \pm k_3. \tag{7}$$

Dyachenko and Zakharov [19] described the general families of such types of resonances. In our case this leads to only one family of resonances, namely

$$k_1 = -a, \qquad k_2 = 9a, \qquad k_3 = 4a, \qquad \text{for} \quad a \in \mathbb{Z}^*.$$

For simplicity of the exposition, the modes will be denoted by a_j instead of a_{k_j} for $j = 1, 2, 3$ and a_{-j} instead of a_{-k_j}.

It is clear from equation (6) that such resonances are built from central carriers, a_3 and a_{-3}, and two equally distant side bands.

Following [18], we perform a canonical transformation from the variables a_j to the variables b_j such that the Hamiltonian is mapped into its normal form.

The Hamiltonian of the system becomes, in the variables b_j,

$$\begin{aligned} H = {} & \sum_{j=1,2,3} \omega_j(|b_j|^2 + |b_{-j}|^2) + \sum_{j=1,2,3} U_j(|b_j|^4 + |b_{-j}|^4 - 4|b_j|^2|b_{-j}|^2) \\ & + V_{21}(|b_2|^2|b_1|^2 + |b_{-2}|^2|b_{-1}|^2) + V_{-21}(|b_2|^2|b_{-1}|^2 + |b_{-2}|^2|b_1|^2) \\ & + V_{31}(-|b_3|^2|b_1|^2 - |b_{-3}|^2|b_{-1}|^2) + V_{-31}(|b_3|^2|b_{-1}|^2 + |b_{-3}|^2|b_1|^2) \\ & + V_{23}(|b_2|^2|b_3|^2 + |b_{-2}|^2|b_{-3}|^2) + V_{-23}(-|b_2|^2|b_{-3}|^2 - |b_{-2}|^2|b_3|^2) \\ & + \tfrac{1}{2}W\big(b_1 b_2 b_3^{*2} + b_1^* b_2^* b_3^2 + b_{-1} b_{-2} b_{-3}^{*2} + b_{-1}^* b_{-2}^* b_{-3}^2\big), \end{aligned} \tag{8}$$

where the coefficients U_j, V_{ij} and W are positive.

The equations of motion are

$$\frac{\mathrm{d}b_j}{\mathrm{d}t} = -\mathrm{i}\frac{\partial H}{\partial b_j^*},$$

for $j = -1, -2, -3, 1, 2, 3$.

We note that, in the infinite-dimensional case, as shown by Dyachenko and Zakharov [19] and Craig and Worfolk [20], the canonical transformation that eliminates the cubic terms also cancels the fourth-order terms. Therefore, the corresponding truncated model happens to be integrable. This property is probably due to a hidden symmetry of the truncation. However, the generic non-integrability should be recovered at some level of the truncation of the normal form since the infinite-dimensional model is certainly not integrable. In our case, starting from the finite-dimensional truncation, the Benjamin–Feir fourth-order terms are instead present in the normal form. We will see that our fourth-order model immediately recovers the generic non-integrability of the initial infinite-dimensional model. In this sense, it might be considered at least as the simplest finite-dimensional model which mimics some crucial features of the full Zakharov model.

Finally, it is worth noting that our model also preserves the time-reversal symmetry of the infinite dimensional one.

A similar Hamiltonian model for fluid interfaces has been derived in [16] where Benjamin–Feir resonances appear even in the infinite-dimensional case due to the presence of the non-vanishing density of the upper fluid.

Using some scaling relations, it is possible to assume that $\omega_1 = 1$, $\omega_2 = 3$ and $\omega_3 = 2$. Indeed, if we rescale the variables b_j by a factor $\sqrt{\lambda}$ for $\lambda \in \mathbb{R}^{*+}$, i.e., if we replace the Hamiltonian $H(b_j, b_j^*)$ by $\lambda H(b_j/\sqrt{\lambda}, b_j^*/\sqrt{\lambda})$ which is a transformation that preserves the equations of motion, and if we rescale time by the same factor λ, i.e., we multiply the Hamiltonian by λ, then it is easy to see that the quartic part of the Hamiltonian is unchanged and the quadratic part is multiplied by λ. By choosing $\lambda = 1/\sqrt{g|a|}$, it means that we can consider that the frequencies are $\omega_1 = 1$, $\omega_2 = 3$ and $\omega_3 = 2$ without loss of generality.

As we shall see, the existence of several integrals of the motion in our system, despite the fact that they are not sufficient to turn it into an integrable one, allows us to reduce the number of degrees of freedom from six to two and to have important information about the dynamics in phase space.

The equations of evolution of $|b_1|^2$, $|b_2|^2$ and $|b_3|^2$ are

$$\begin{aligned}
\frac{\mathrm{d}}{\mathrm{d}t}|b_1|^2 &= \mathrm{i}\frac{W}{2}\left(b_1 b_2 b_3^{*2} - b_1^* b_2^* b_3^2\right),\\
\frac{\mathrm{d}}{\mathrm{d}t}|b_2|^2 &= \mathrm{i}\frac{W}{2}\left(b_1 b_2 b_3^{*2} - b_1^* b_2^* b_3^2\right),\\
\frac{\mathrm{d}}{\mathrm{d}t}|b_3|^2 &= -\mathrm{i}W\left(b_1 b_2 b_3^{*2} - b_1^* b_2^* b_3^2\right).
\end{aligned}$$

Therefore, we see that the following two quantities are conserved:

$$\mathbb{I}_+ = 2|b_1|^2 + |b_3|^2, \tag{9}$$

$$\mathbb{J}_+ = |b_1|^2 + 3|b_2|^2 + 2|b_3|^2. \tag{10}$$

In what follows, we will also use a linear combination of these two conserved quantities

$$\mathbb{K}_+ = |b_1|^2 - |b_2|^2 = \tfrac{1}{3}(2\mathbb{I}_+ - \mathbb{J}_+). \tag{11}$$

By defining $N_j \equiv |b_j|^2$ for $j = 1, 2, 3$, the constants of motion become

$$\mathbb{I}_+ = 2N_1 + N_3, \qquad \mathbb{J}_+ = N_1 + 3N_2 + 2N_3.$$

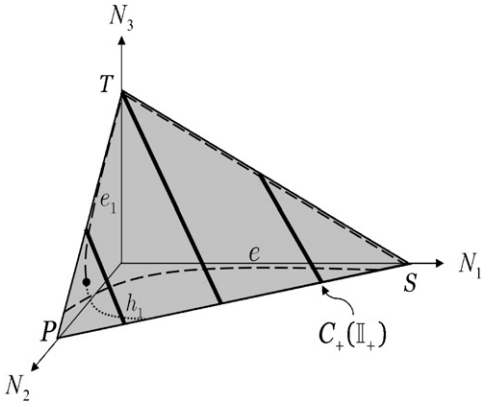

Figure 1. Representation of the phase space $\mathbb{E}_+$ and the three families of fixed points found on the (N_1, θ_1) plane. The location of the elliptic points $e(\mathbb{I}_+)$, $e_1(\mathbb{I}_+)$ is represented by a dashed line. The location of the hyperbolic points $h_1(\mathbb{I}_+)$ is represented by a dotted line. The bifurcation creating the pair of elliptic/hyperbolic $e_1(\mathbb{I}_+)/h_1(\mathbb{I}_+)$ point is indicated by a dot.

Similarly, we have two additional conserved quantities for the other resonance

$$\mathbb{I}_- = 2N_{-1} + N_{-3}, \qquad \mathbb{J}_- = N_{-1} + 3N_{-2} + 2N_{-3},$$

where $N_{-j} \equiv |b_{-j}|^2$ for $j = 1, 2, 3$.

It can be checked that the four integrals $\mathbb{I}_+, \mathbb{J}_+, \mathbb{I}_-, \mathbb{J}_-$ are independent and in involution. The key point to be noted here is the fact that each one of these first integrals depends on the variables of one resonance alone even if, as will be seen, there is a dynamical interaction of the two sets of variables.

Let us now look at the structure of the invariant surfaces in phase space in view of the previous integrals of motion. Even if they cannot completely fix the orbits of the system, they help to understand many properties of the different dynamical regimes observed in this model.

In the space $\mathbb{E}_+ = (N_1, N_2, N_3)$ (respectively $\mathbb{E}_- = (N_{-1}, N_{-2}, N_{-3})$), $\mathbb{J}_+ = \text{const}$ (resp. $\mathbb{J}_- = \text{const}$) defines a portion of a plane that we represent in figure 1. On the other hand, the intersection of this set with $\mathbb{I}_+ = \text{const}$ (resp. $\mathbb{I}_- = \text{const}$) defines a family of segments $C_+(\mathbb{I}_+)$ (resp. $C_-(\mathbb{I}_-)$).

Let us consider the structure of $\mathbb{E}_+$ and let us fix $\mathbb{J}_+ \neq 0$. For $\mathbb{I}_+ = 0$, the set $C_+(0)$ reduces to one point P whose coordinates are $P = (0, \mathbb{J}_+/3, 0)$.

For $0 < \mathbb{I}_+ < \frac{\mathbb{J}_+}{2}$, the intersection of the two invariant surfaces in $\mathbb{E}_+$, $C_+(\mathbb{I}_+)$ is a segment close to P.

When $\mathbb{I}_+ = \mathbb{J}_+/2$, $C_+(\mathbb{J}_+/2)$ is a segment with one extremity $T = (0, 0, \mathbb{J}_+/2)$. We note that on this curve we have $N_1 = N_2$.

For $\mathbb{J}_+/2 < \mathbb{I}_+ < 2\mathbb{J}_+$, the set $C_+(\mathbb{I}_+)$ is a segment close to $S = (\mathbb{J}_+, 0, 0)$.

For $\mathbb{I}_+ = 2\mathbb{J}_+$, the intersection is the point S.

For $\mathbb{I}_+ > 2\mathbb{J}_+$ or for $\mathbb{I}_+ < 0$ the intersection is empty.

We note that $\mathbb{E}_+ \times \mathbb{E}_-$ needs to be supplemented by additional variables like the six angles Φ_j of the complex variables b_j in order to build the phase space. Therefore, since the projection of an orbit on $\mathbb{E}_+ \times \mathbb{E}_-$ alone is only part of the information we must look at it as partial, although useful, information on the dynamics. This is why, in each case we shall supplement its description with additional information in order to make a complete characterization of the dynamics.

Remark 1. In the derivation of the Hamiltonian (8), when two modes of each resonance are equal to zero, e.g., $b_j = b_{-j} = 0$ for $j = 1, 3$, then $a_2 = b_2 + 2\widetilde{V}^{(4)}_{2,2,-2,-2} b^{*2}_{-2} b^*_2$.

Furthermore, the transformation which maps $\{a_j\}$ into $\{b_j\}$ is canonical, i.e., it satisfies

$$\sum_j \mathrm{i}\,\mathrm{d}b_j \wedge \mathrm{d}b^*_j = \sum_j \mathrm{i}\,\mathrm{d}a_j \wedge \mathrm{d}a^*_j. \tag{12}$$

Remark 2. The derivation of Hamiltonian (8) can also be done by considering the nonlinear Schrödinger equation (as it is used for instance in [21]):

$$\mathrm{i}(\partial_t \psi + c\partial_x \psi) = \nu \partial_x^2 \psi + \mu |\psi|^2 \psi,$$

and by considering that ψ only contains the selected modes we consider in this paper:

$$\psi = \psi_{-3}(t)\,\mathrm{e}^{\mathrm{i}k_{-3}x} + \psi_{-2}(t)\,\mathrm{e}^{\mathrm{i}k_{-2}x} + \psi_{-1}(t)\,\mathrm{e}^{\mathrm{i}k_{-1}x} + \psi_1(t)\,\mathrm{e}^{\mathrm{i}k_1 x} + \psi_2(t)\,\mathrm{e}^{\mathrm{i}k_2 x} + \psi_3(t)\,\mathrm{e}^{\mathrm{i}k_3 x}.$$

Using a Galerkin truncation, one arrives at a Hamiltonian expressed in the a_k-like variables. By a normal form expansion very similar to the one we used to derive Hamiltonian (8), one arrives at the same expression for the Hamiltonian (8) in terms of the b_k-like variables.

3. Dynamics with one resonance

To get insight into the full dynamics, we begin with simple and integrable situations which will allow us to understand the general case with two resonances. We start exploring the phase space by choosing initial conditions leading to simple situations for which we can exhibit different kinds of shapes of the wave. A complete description of phase space is given by a numerical analysis.

It follows from the conserved quantities that an orbit corresponding to an initial condition with all null coordinates in one of the two resonance variables N_j will keep this property for any time. For instance, we assume that $\mathbb{J}_- = 0$. This implies that $N_{-1} = N_{-2} = N_{-3} = 0$ for all time. Thus, we first study the dynamics with only one resonance which is an integrable case since Hamiltonian (13) has three degrees of freedom and three conserved quantities (e.g., $H, \mathbb{I}_+, \mathbb{K}_+$). Hamiltonian (8) describing the dynamics in the variables (b_1, b_2, b_3) becomes

$$\begin{aligned} H = {} & |b_1|^2 + 3|b_2|^2 + 2|b_3|^2 + U_1|b_1|^4 + U_2|b_2|^4 + U_3|b_3|^4 + V_{21}|b_2|^2|b_1|^2 - V_{31}|b_3|^2|b_1|^2 \\ & + V_{23}|b_2|^2|b_3|^2 + \tfrac{1}{2}W\left(b_1 b_2 b^{*2}_3 + b^*_1 b^{*2}_2 b^2_3\right). \end{aligned} \tag{13}$$

In what follows, we describe the dynamics on the sets $C_+(\mathbb{I}_+)$ described in the previous section (see figure 1). We start with the simplest cases which are the three points P, T and S and the segment (PS) (one of the boundaries of the triangle $\mathbb{E}_+$) for which we can exhibit analytical expressions for the shape of the wave $\eta(x, t)$.

3.1. Dynamics of orbits of P, T, S

First, we consider the orbits corresponding to the point P of $\mathbb{E}_+$ (where $\mathbb{I}_+ = 0$). The equations of motion read

$$\begin{aligned} & N_1 \equiv |b_1|^2 = 0, \qquad && N_3 \equiv |b_3|^2 = 0, \\ & N_2 \equiv |b_2|^2 = \frac{\mathbb{J}_+}{3}, \qquad && \mathrm{i}\frac{\mathrm{d}b_2}{\mathrm{d}t} = (3 + 2U_2|b_2|^2)b_2. \end{aligned}$$

The solution in the variables b_j is then

$$\begin{aligned} & b_2(t) = \sqrt{\frac{\mathbb{J}_+}{3}} \exp\left(-\mathrm{i}\left(3 + 2U_2\frac{\mathbb{J}_+}{3}\right)t - \mathrm{i}\Phi\right), \\ & b_j(t) = 0, \qquad \text{for} \quad j = 1, 3. \end{aligned} \tag{14}$$

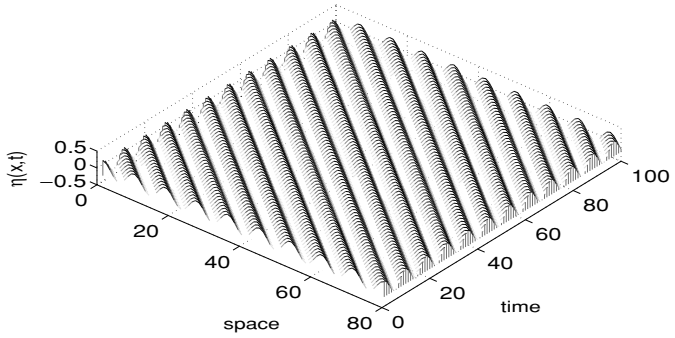

Figure 2. Elevation of the surface $\eta(x, t)$ corresponding to $P(\mathbb{I}_+ = 0)$ for Hamiltonian (13) with one resonance.

Therefore, for any $\mathbb{J}_+ > 0$ these orbits are periodic in time. Since we have only one resonance, the original variables a_j are equal to b_j.

Thus, the expression for the shape of the wave is

$$\eta(x, t) = \frac{\sqrt{3}g^{-1/4}}{2\pi\sqrt{2}}(b_2(t)\exp(9\mathrm{i}x) + b_2^*(t)\exp(-9\mathrm{i}x)), \tag{15}$$

which is also

$$\eta(x, t) = \eta_0\cos(9(x - c_2t) + \phi), \tag{16}$$

i.e., travelling waves with velocity

$$c_2 = \frac{1}{3} + \frac{4\pi^2}{9}\sqrt{g}U_2{\eta_0}^2. \tag{17}$$

A plot of the shape of this wave is represented in figure 2.

Similarly for S, we obtain travelling waves running backwards $\eta(x, t) = \eta_0\cos(x + c_1t + \phi)$ with velocity

$$c_1 = 1 + 4\pi^2\sqrt{g}U_1{\eta_0}^2.$$

For T, we obtain travelling waves running forwards $\eta(x, t) = \eta_0\cos(4(x - c_3t) + \phi)$ with velocity

$$c_3 = \tfrac{1}{2} + \pi^2\sqrt{g}U_3{\eta_0}^2.$$

A linear stability of the points P, S and T shows that these fixed points of the dynamics are elliptic. It means that nearby trajectories will mimic the behaviour of the dynamics of these points. In particular, the surface waves near these points are time quasiperiodic waves close to travelling waves.

3.2. Dynamics on a point on the segment (PS)

We consider the point which is at the intersection of $C_+(\mathbb{I}_+)$ and the segment (PS), for a value of $\mathbb{I}_+ \in [0, 2\mathbb{J}_+]$. This point is such that $b_3(0) = 0$ and $\mathrm{d}b_3(0)/\mathrm{d}t = 0$. From the equation for $b_3(t)$, we deduce that $b_3(t) = 0$ for any time. From the two invariants $\mathbb{I}_+$ and $\mathbb{J}_+$, we have that N_1 and N_2 are constant and equal to $N_1(t) = \mathbb{I}_+/2$ and $N_2(t) = (2\mathbb{J}_+ - \mathbb{I}_+)/6$. The equations of motion become

$$\frac{\mathrm{d}b_1}{\mathrm{d}t} = -\mathrm{i}\left(1 + \left(U_1 - \frac{V_{21}}{6}\right)\mathbb{I}_+ + \frac{V_{21}}{3}\mathbb{J}_+\right)b_1,$$

$$\frac{\mathrm{d}b_2}{\mathrm{d}t} = -\mathrm{i}\left(3 + \left(-\frac{U_2}{3} + \frac{V_{21}}{2}\right)\mathbb{I}_+ + \frac{2}{3}V_{21}\mathbb{J}_+\right)b_2.$$

We deduce the expressions for b_1 and b_2:

$$\begin{aligned} b_1(t) &= \sqrt{\frac{\mathbb{I}_+}{2}} \exp\left(-\mathrm{i}\left[1 + \left(U_1 - \frac{V_{21}}{6}\right)\mathbb{I}_+ + \frac{V_{21}}{3}\mathbb{J}_+\right]t + \alpha_1\right), \\ &= \sqrt{\frac{\mathbb{I}_+}{2}} \exp\left[-\mathrm{i}(c_1 t + \alpha_1)\right], \\ b_2(t) &= \sqrt{(2\mathbb{J}_+ - \mathbb{I}_+)/6} \exp\left(-\mathrm{i}\left[3 + \left(-\frac{U_2}{3} + \frac{V_{21}}{2}\right)\mathbb{I}_+ + \frac{2}{3}V_{21}\mathbb{J}_+\right]t + \alpha_2\right), \\ &= \sqrt{\frac{2\mathbb{J}_+ - \mathbb{I}_+}{6}} \exp\left[-\mathrm{i}(9c_2 t + \alpha_2)\right], \end{aligned}$$

where $c_1 = 1 + (U_1 - V_{21}/6)\mathbb{I}_+ + V_{21}/3\mathbb{J}_+$ and $c_2 = [3 + (-U_2/3 + V_{21})\mathbb{I}_+ + 2/3V_{21}\mathbb{J}_+]/9$. The expression for the shape of the wave is

$$\eta(x,t) = \frac{g^{-1/4}}{2\pi}(\sqrt{\mathbb{I}_+}\cos(x + c_1 t + \alpha_1) + \sqrt{2\mathbb{J}_+ - \mathbb{I}_+}\cos(9(x - c_2 t) + \alpha_2)),$$

which is the sum of two travelling waves with two different velocities.

We note that on P (respectively on S), the amplitude of the travelling wave with velocity c_1 (respectively c_2) vanishes. Therefore, the wave associated with P (respectively S) becomes the travelling wave with velocity c_2 (respectively c_1) obtained in section 3.1.

3.3. Dynamics of orbits on $C_+(\mathbb{I}_+)$

Next, we extend the dynamics with one resonance, by studying the dynamics on the full sets $C_+(\mathbb{I}_+)$ for $\mathbb{I}_+ \in [0, 2\mathbb{J}_+]$. We determine numerically the profiles of the waves which are similar to those obtained previously, namely stationary, travelling, time periodic and quasiperiodic waves. This study also gives all the information about the exchanges of energy which occur between the modes.

In order to study the orbits in this case, since we have a Hamiltonian with three degrees of freedom and three constants of motion, we want to perform a canonical change of variables reducing the dimension of the system to one degree of freedom. Furthermore, we would like to change canonically the coordinates into action-angle variables (N_j, Φ_j) such that $b_j = \sqrt{N_j}\,\mathrm{e}^{-\mathrm{i}\Phi_j}$.

First, we note that if $N_3(0) = 0$, then $N_3(t) = 0$ at any time t (see section 3.2). In what follows, we always exclude this point which is at the intersection of (PS) and $C_+(\mathbb{I}_+)$.

In the case where $\mathbb{I}_+ = \mathbb{J}_+/2$, we note that since $\mathbb{K}_+ = N_1 - N_2$ is a conserved quantity (equal to zero in this case), if N_1 vanishes at some time, then N_2 also vanishes. This dynamics occurs at the point T (see section 3.1). Except this particular case, there are two interesting cases where $\mathbb{I}_+ > \mathbb{J}_+/2$ and $\mathbb{I}_+ < \mathbb{J}_+/2$. If $\mathbb{I}_+ < \mathbb{J}_+/2$, only N_1 vanishes since $N_2 \geqslant (\mathbb{J}_+ - 2\mathbb{I}_+)/3 > 0$. If $\mathbb{I}_+ > \mathbb{J}_+/2$, only N_2 vanishes since $N_1 \geqslant (2\mathbb{I}_+ - 2\mathbb{J}_+)/3 > 0$.

We remark that N_1 is such that $\max(0, \mathbb{K}_+) \leqslant N_1 \leqslant \mathbb{I}_+/2$, so the accessible phase space in the $(p_1, q_1) = (\mathrm{Re}(b_1), \mathrm{Im}(b_1))$-plane is a circle for $\mathbb{K}_+ < 0$ and an annulus for $\mathbb{K}_+ > 0$.

In order to avoid the two cases $N_1 = 0$ or $N_2 = 0$ for which the angle ϕ_1 or ϕ_2 is not defined in the change of variables, we first show that there is only one trajectory $\mathcal{T}_1$ such that $N_1(t) = 0$, i.e., which passes by zero in the (p_1, q_1)-plane.

First, we note that Hamilton's equations associated with Hamiltonian (13) are invariant by the two transformations:

$$\hat{b}_1 = b_1, \qquad \hat{b}_2 = b_2\,\mathrm{e}^{-\mathrm{i}\phi}, \qquad \hat{b}_3 = b_3\,\mathrm{e}^{-\mathrm{i}\phi/2},$$

and

$$\hat{b}_1 = b_1 \, \mathrm{e}^{-\mathrm{i}\phi}, \qquad \hat{b}_2 = b_2, \qquad \hat{b}_3 = b_3 \, \mathrm{e}^{-\mathrm{i}\phi/2},$$

where ϕ is constant. Using these two invariants, one can show that there is basically one trajectory $\mathcal{T}_1$ which passes by zero in the (p_1, q_1)-plane. The closed trajectory $\mathcal{T}_1$ divides the phase space in the (p_1, q_1)-plane into two parts: the inside and the outside of $\mathcal{T}_1$.

Similarly, for $\mathbb{K}_+ > 0$, there is only one trajectory $\mathcal{T}_2$ which passes by zero in (p_2, q_2)-plane.

We note that $N_2 = 0$ corresponds to $N_1 = \mathbb{K}_+$ and so a trajectory which passes by zero in the (p_2, q_2)-plane is a trajectory which passes by the point $N_1 = \mathbb{K}_+$ in the (p_1, q_1)-plane, which is the inside border of the accessible region.

The trajectory $\mathcal{T}_2$ divides the annulus into two parts: the inside and the outside of $\mathcal{T}_2$. Thus, in either of these two parts, N_1 and N_2 are strictly positive.

In the regions where all actions N_1, N_2 and N_3 are strictly positive, we perform a canonical transformation that expresses Hamiltonian (13) into action-angle variables:

$$b_j = \sqrt{N_j} \, \mathrm{e}^{-\mathrm{i}\Phi_j}. \tag{18}$$

This transformation is canonical, i.e.,

$$\sum_{j=1,2,3} \mathrm{i} \, \mathrm{d}b_j \wedge \mathrm{d}b_j^* = \sum_{j=1,2,3} \mathrm{d}N_j \wedge \mathrm{d}\Phi_j.$$

The actions N_1, N_2, N_3 are, respectively, conjugate to the angles Φ_1, Φ_2, Φ_3. Hamiltonian (13) becomes

$$\begin{aligned} H = {} & N_1 + 3N_2 + 2N_3 + U_1 N_1^2 + U_2 N_2^2 + U_3 N_3^2 + V_{21} N_1 N_2 - V_{31} N_1 N_3 + V_{23} N_2 N_3 \\ & + W \sqrt{N_1 N_2} N_3 \cos(\Phi_1 + \Phi_2 - 2\Phi_3). \end{aligned} \tag{19}$$

Hamilton's equations for Hamiltonian (19) are given by

$$\frac{\mathrm{d}\Phi_j}{\mathrm{d}t} = \frac{\partial H}{\partial N_j}, \qquad \frac{\mathrm{d}N_j}{\mathrm{d}t} = -\frac{\partial H}{\partial \Phi_j},$$

for $j = 1, 2, 3$.

Using the invariants $\mathbb{I}_+$ and $\mathbb{J}_+$, we now proceed to the reduction of the dimension of the system to one degree of freedom.

We perform the following canonical transformation from $(N_1, N_2, N_3, \Phi_1, \Phi_2, \Phi_3)$ to $(\tilde{N}_1, \mathbb{K}_+, \mathbb{I}_+, \theta_1, \theta_2, \theta_3)$:

$$\begin{aligned} & \tilde{N}_1 = N_1, && \mathbb{K}_+ = N_1 - N_2, && \mathbb{I}_+ = 2N_1 + N_3, \\ & \theta_1 = \Phi_1 + \Phi_2 - 2\Phi_3, && \theta_2 = -\Phi_2, && \theta_3 = \Phi_3. \end{aligned} \tag{20}$$

The actions $\tilde{N}_1, \mathbb{K}_+$ and $\mathbb{I}_+$ are now, respectively, conjugate to angles θ_1, θ_2 and θ_3. In what follows, we use N_1 instead of $\tilde{N}_1$ for simplicity. Hamiltonian (19) becomes

$$H = \Omega_0 + \Omega_1 N_1 + \Omega_2 N_1^2 + W \sqrt{N_1} \sqrt{N_1 - \mathbb{K}_+} (\mathbb{I}_+ - 2N_1) \cos\theta_1, \tag{21}$$

where the functions Ω_0 and Ω_1 only depend on the actions $\mathbb{I}_+, \mathbb{K}_+$, and Ω_2 is constant:

$$\begin{aligned} \Omega_0 &= -3\mathbb{K}_+ + 2\mathbb{I}_+ + U_3 \mathbb{I}_+^2 + U_2 \mathbb{K}_+^2 - V_{23} \mathbb{I}_+ \mathbb{K}_+, \\ \Omega_1 &= -2U_2 \mathbb{K}_+ - 4U_3 \mathbb{I}_+ - V_{21} \mathbb{K}_+ - V_{31} \mathbb{I}_+ + V_{23} (\mathbb{I}_+ + 2\mathbb{K}_+), \\ \Omega_2 &= U_1 + U_2 + 4U_3 + V_{21} + 2V_{31} - 2V_{23}. \end{aligned} \tag{22}$$

We note that Hamiltonian (21) does not depend on the angles θ_2 and θ_3 which is equivalent to saying that $\mathbb{I}_+$ and $\mathbb{K}_+$ are invariant (constants of motion).

In order to visualize the dynamics, we perform numerical integration of the equations of motion associated with Hamiltonian (21).

A plot of some trajectories for $\mathbb{J}_+ = 1$ and different values of $\mathbb{I}_+$ in the accessible region of the phase space (grey region) is given in figure 3. In these plots, we have transformed from action-angle (N_1, θ_1) to Cartesian coordinates $P_1 = \sqrt{N_1}\cos\theta_1$, $Q_1 = \sqrt{N_1}\sin\theta_1$. In these last variables, the accessible region is, for $\mathbb{K}_+ < 0$, i.e. $\mathbb{I}_+ < \mathbb{J}_+/2$, the set of points in the interior of the circle $N_1 = \mathbb{I}_+/2$ and such that these points are inside $\mathcal{T}_1$ or outside $\mathcal{T}_1$ (where the canonical transformation from the original variables b_j to action-angle variables (N_j, θ_j) is well defined). For $\mathbb{K}_+ > 0$, i.e. $\mathbb{I}_+ > \mathbb{J}_+/2$, the accessible region is the annulus $\mathbb{K}_+ < N_1 < \mathbb{I}_+/2$ and such that these points are inside $\mathcal{T}_2$ or outside $\mathcal{T}_2$.

Below, we see that these plots are characterized by elliptic, hyperbolic points and the associated separatrices. We discuss the location of these points with respect to the parameter $\mathbb{I}_+$.

The fixed points are obtained when $\dot{N}_1 = 0$ and $\dot{\theta}_1 = 0$. As depicted in figure 1, there is three families of fixed points. The first family, denoted $e(\mathbb{I}_+)$, is located at $\theta_1 = 0$ and is elliptic. Its position N_1 is a solution of the equation:

$$\Omega_1 + 2\Omega_2 N_1 + \frac{W}{2}\left[\left(\sqrt{\frac{N_1 - \mathbb{K}_+}{N_1}} + \sqrt{\frac{N_1}{N_1 - \mathbb{K}_+}}\right)(\mathbb{I}_+ - 2N_1) - 4\sqrt{N_1(N_1 - \mathbb{K}_+)}\right] = 0, \tag{23}$$

which is the equation of $\dot{\theta}_1 = 0$ for $\theta_1 = 0$.

There exist two other families of fixed points located at $\theta_1 = \pi$, one an elliptic point denoted by $e_1(\mathbb{I}_+)$ and the other a hyperbolic point denoted by $h_1(\mathbb{I}_+)$.

The location N_1 is given by the equation

$$\Omega_1 + 2\Omega_2 N_1 - \frac{W}{2}\left[\left(\sqrt{\frac{N_1 - \mathbb{K}_+}{N_1}} + \sqrt{\frac{N_1}{N_1 - \mathbb{K}_+}}\right)(\mathbb{I}_+ - 2N_1) - 4\sqrt{N_1(N_1 - \mathbb{K}_+)}\right] = 0, \tag{24}$$

which is the equation of $\dot{\theta}_1 = 0$ for $\theta_1 = \pi$.

The location of all these fixed points as a function of $\mathbb{I}_+$ is depicted in figure 1.

We see in the different plots in figure 3 that when $\mathbb{I}_+$ is close to zero, there are no fixed points. When we increase $\mathbb{I}_+$ there is only one elliptic fixed point $e(\mathbb{I}_+)$ (figure 3(a)) which appears near zero. As the value of $\mathbb{I}_+$ increases, there are three fixed points: besides the previous elliptic fixed point $e(\mathbb{I}_+)$, there is a bifurcation (fold, which is structurally stable) where two new fixed points appear, an elliptic point $e_1(\mathbb{I}_+)$ and a hyperbolic one $h_1(\mathbb{I}_+)$ (figure 3(b)).

We have a homoclinic connection for the hyperbolic fixed point. When the value of $\mathbb{I}_+$ still increases and remains lower than $\mathbb{J}_+/2$, the elliptic fixed point $e(\mathbb{I}_+)$ moves to the right and the hyperbolic one $h_1(\mathbb{I}_+)$ moves to the left, both going towards the border of the phase space. At the same time, the elliptic fixed point $e_1(\mathbb{I}_+)$ moves to the right going to the centre of the phase space so approaching $N_1 = 0$. When $\mathbb{I}_+$ is close to $\mathbb{J}_+/2$, the elliptic fixed point $e_1(\mathbb{I}_+)$ remains near the border $N_1 = 0$ but it is not apparent in the figures and the hyperbolic one $h_1(\mathbb{I}_+)$ remains near the border $N_1 = \mathbb{I}_+/2$ (figure 3(c)).

For $\mathbb{I}_+ > \mathbb{J}_+/2$, the hyperbolic point $h_1(\mathbb{I}_+)$ remains at the border $N_1 = \mathbb{I}_+/2$ and the elliptic point $e_1(\mathbb{I}_+)$ is in the border of the annulus where $\mathbb{K}_+ > 0$. At the same time, the region

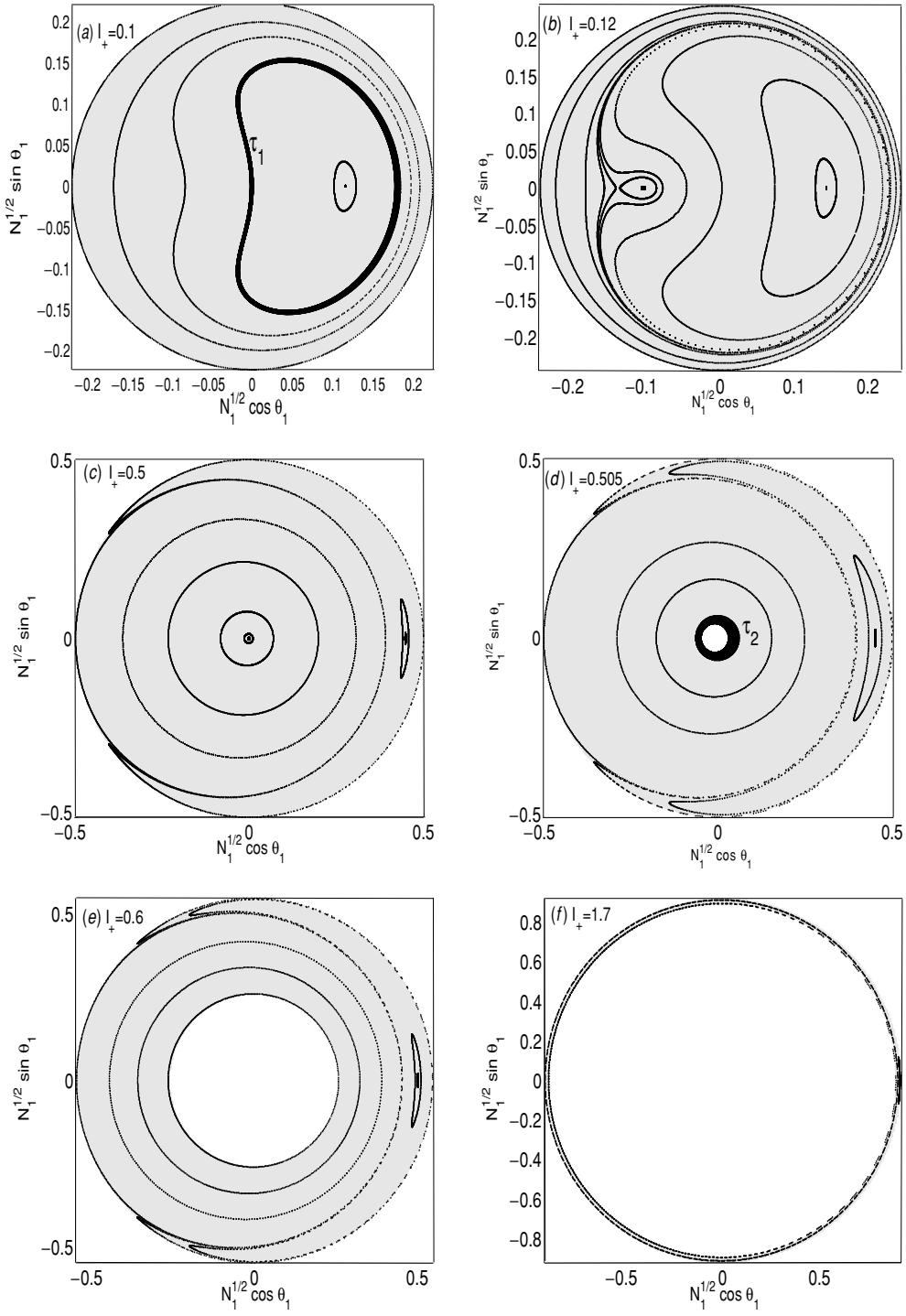

Figure 3. Phase space trajectories of Hamiltonian (13) with one resonance for different values of $\mathbb{I}_+$: (*a*) $\mathbb{I}_+ = 0.1$, (*b*) $\mathbb{I}_+ = 0.12$, (*c*) $\mathbb{I}_+ = 0.5$, (*d*) $\mathbb{I}_+ = 0.505$, (*e*) $\mathbb{I}_+ = 0.6$, (*f*) $\mathbb{I}_+ = 1.7$. The grey region is the accessible region of phase space: which is the annulus $\max(0, \mathbb{K}_+) \leqslant N_1 \leqslant \mathbb{I}_+/2$. The bold curve $\mathcal{T}_1$ represents the trajectory which passes by $N_1 = 0$.

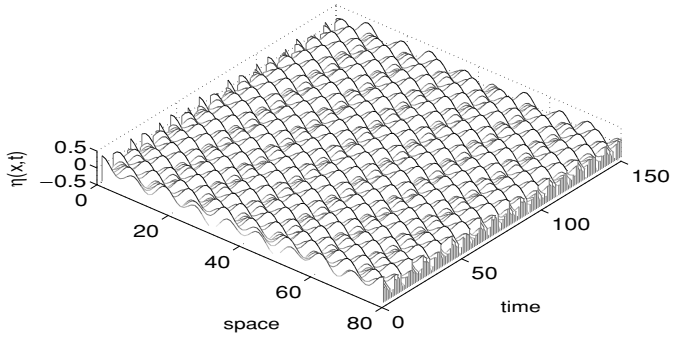

Figure 4. Elevation of the surface $\eta(x,t)$ for Hamiltonian (13) with one resonance for $\mathbb{J}_+ = 1$, $\mathbb{I}_+ = \mathbb{J}_+/2$ and for the fixed point $e(\mathbb{J}_+/2)$.

in which N_1 evolves decreases (figures 3(*d*) and (*e*)). For $\mathbb{I}_+$ near $2\mathbb{J}_+$, the phase space merges to the point S.

We note that for $\mathbb{I}_+ = \mathbb{J}_+/2$, the resonance occupies a larger region of phase space than the other cases. This is in agreement with figure 1. All these fixed points correspond to periodic variations in variables N_1, N_2, N_3 and Φ_1, Φ_2, Φ_3. Indeed, due to the invariants given by equations (9) and (10), if N_1 is fixed, N_2 and N_3 remain fixed and the angles Φ_1, Φ_2, Φ_3 evolve linearly in time. For example, in the case $\mathbb{I}_+ = \mathbb{J}_+/2$ (i.e., $\mathbb{K}_+ = 0$), we give explicitly the dynamics corresponding to $e(\mathbb{J}_+/2)$. The equations of motion are

$$\begin{aligned} \frac{\mathrm{d}N_1}{\mathrm{d}t} &= WN_1(\mathbb{I}_+ - 2N_1)\sin\theta_1, \\ \frac{\mathrm{d}\theta_1}{\mathrm{d}t} &= \Omega_1 + W\mathbb{I}_+\cos\theta_1 + 2N_1(\Omega_2 - 2W\cos\theta_1). \end{aligned} \tag{25}$$

For $\theta_1 = 0$ and

$$N_1 = \frac{\Omega_1 + W\mathbb{I}_+}{-2\Omega_2 + 4W}, \tag{26}$$

we get an elliptic fixed point with $N_1 \leqslant \mathbb{I}_+/2$ for all $\mathbb{I}_+ = \mathbb{J}_+/2$. This means that this fixed point exists for all admissible values of the parameter $\mathbb{J}_+$ and for $\mathbb{I}_+ = \mathbb{J}_+/2$.

We deduce the expressions of the linear motion of the angles:

$$\begin{aligned} \Phi_1(t) &= \left[1 - V_{31}\mathbb{I}_+ + \tfrac{1}{2}W\mathbb{I}_+ + (2U_1 + V_{21} - 2V_{31} - W)N_1\right]t + \Phi_1(0), \\ &= c_1 t + \alpha_1, \\ \Phi_2(t) &= \left[3 + V_{23}\mathbb{I}_+ + \tfrac{1}{2}W\mathbb{I}_+ + (V_{21} + 2U_2 - 2V_{23} - W)N_1\right]t + \Phi_2(0), \\ &= 9c_2 t + \alpha_2, \\ \Phi_3(t) &= [2 + 2U_3\mathbb{I}_+ + (-V_{31} + V_{23} - 4U_3 + W)N_1]\,t + \Phi_3(0), \\ &= 4c_3 t + \alpha_3. \end{aligned}$$

This linear dynamics gives the following shape of the wave:

$$\begin{aligned} \eta(x,t) = \frac{g^{-1/4}}{\pi\sqrt{2}}&(\sqrt{N_1}\cos(x + c_1 t + \alpha_1) + \sqrt{3}\sqrt{N_1}\cos[9(x - c_2 t) + \alpha_2] \\ &+ \sqrt{2}\sqrt{\mathbb{I}_+ - 2N_1}\cos[4(x - c_3 t) + \alpha_3]), \end{aligned} \tag{27}$$

which is a sum of three travelling waves with different velocities.

For this case, we have plotted in figure 4 the elevation of the surface $\eta(x,t)$. We see that η is quasiperiodic in time.

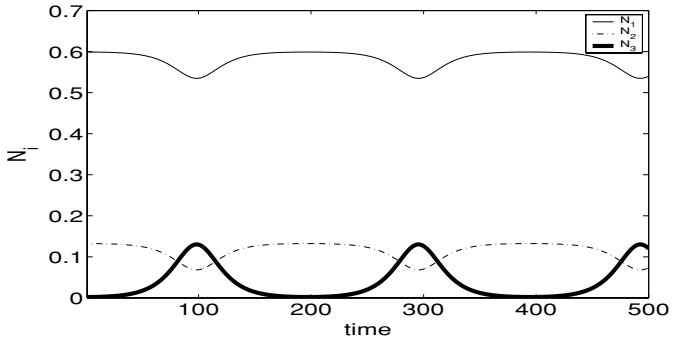

Figure 5. Temporal evolution of modes N_i for $i = 1, 2, 3$, for Hamiltonian (19) with one resonance, $\mathbb{I}_+ = 1.2$, $\mathbb{J}_+ = 1$ and an initial condition $(N_1, \theta_1) = (\mathbb{I}_+/2, \pi)$.

3.4. Exchanges of energy on $C_+(\mathbb{I}_+)$

We will now see how the exchanges of energy occur among the three modes for different values of $\mathbb{I}_+$.

Since all the orbits of $C_+(\mathbb{I}_+)$ are closed, the function $N_1(t)$ is periodic. From the two invariants $\mathbb{I}_+$ and $\mathbb{J}_+$, the two other actions $N_2(t)$ and $N_3(t)$ are periodic with the same period as $N_1(t)$. Therefore, all the exchanges which occur in the system are periodic in time.

- We consider $C_+(\mathbb{I}_+)$ with $\frac{\mathbb{J}_+}{2} < \mathbb{I}_+ < 2\mathbb{J}_+$. Let us first consider the trajectories with initial conditions close to S, i.e., such that $N_2(0)$ and $N_3(0)$ are of order $\varepsilon \ll 1$. If we set $\mathbb{I}_+ = 2\mathbb{J}_+ - \varepsilon$, we get from equations (9) and (10)

$$\frac{\mathbb{I}_+}{2} - \frac{\varepsilon}{6} \leqslant N_1(t) \leqslant \frac{\mathbb{I}_+}{2}, \qquad 0 \leqslant N_2(t) \leqslant \frac{\varepsilon}{6}, \qquad 0 \leqslant N_3(t) \leqslant \frac{\varepsilon}{3},$$

  for all t.

  In fact, this behaviour is valid for all values of $\mathbb{I}_+$. So, if we have initially $N_1(0) \gg N_2(0)$ and $N_3(0)$, then by looking at the invariant $\mathbb{I}_+$, we see that for $N_3(0)$ close to zero, $N_1(t)$ decreases and at the same time $N_3(t)$ increases. The invariant $2N_2 + N_3 \approx 2N_2(0)$ shows that $N_2(t)$ also decreases and $N_3(t)$ does not grow more than $2N_2(0)$ which is small as we can see in figure 5, where we have plotted the time evolution of the amplitudes N_1, N_2 and N_3 for the initial condition $(N_1, \theta_1) = \left(\frac{\mathbb{I}_+}{2}, \pi\right)$.

  Therefore, when almost all the energy is initially carried by the lower frequency mode N_1, the oscillations of the amplitudes are very small and there is no significant energy exchange between the modes.

  By looking directly at figure 1, we also see that, for such values of $\mathbb{I}_+$, only the modes N_2 and N_3 may exchange their energy while N_1 may only sustain small energy fluctuations. In the same way, for an orbit corresponding to $C_+(\mathbb{I}_+)$ with $0 < \mathbb{I}_+ < \mathbb{J}_+/2$, there is no significant energy exchange for initial conditions close to P, and in any case only N_1 and N_3 enable some energy exchange among the modes.
- In order to obtain large energy exchanges between the three modes, we have to put as much energy in the side bands as in the central carrier: the contribution of energy to the side bands is equal to $\omega_1 N_1 + \omega_2 N_2 = N_1 + 3N_2$. The maximum energy exchange is obtained when $N_1 + 3N_2 = 2N_3 = \mathbb{J}_+/2$. This happens in the zone where N_1 and N_2 are equally important, namely close to $C_+(\mathbb{J}_+/2)$.

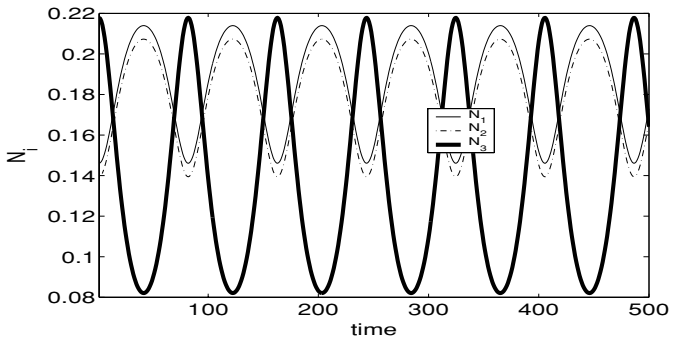

Figure 6. Temporal evolution of modes N_i for $i = 1, 2, 3$, for Hamiltonian (19) with one resonance, $\mathbb{J}_+ = 1$, $\mathbb{I}_+$ in the neighbourhood of $\mathbb{I}_+ = \mathbb{J}_+/2$ and an initial condition $(N_1, \theta_1) = (\mathbb{J}_+/8, 0)$.

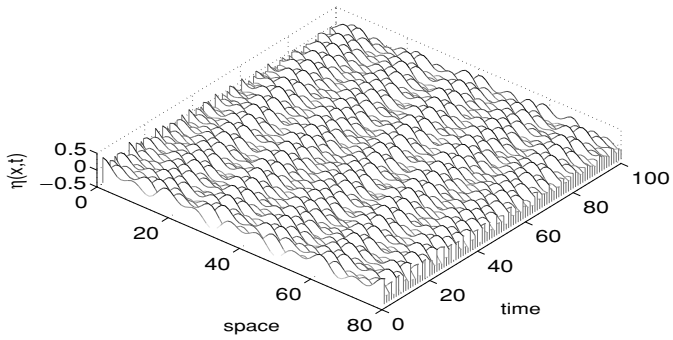

Figure 7. Elevation of the surface $\eta(x, t)$ Hamiltonian (19) with one resonance for $\mathbb{J}_+ = 1$, in the neighbourhood of $\mathbb{I}_+ = \mathbb{J}_+/2$ and an initial condition $(N_1, \theta_1) = (\mathbb{J}_+/8, 0)$.

In this case, using the form of the three integrals of the motion and assuming $\mathbb{I}_+ = \mathbb{J}_+/2 + \varepsilon$, we get

$$0 \leqslant N_3(t) \leqslant \frac{\mathbb{J}_+}{2} + \varepsilon, \qquad \frac{2\varepsilon}{3} \leqslant N_1(t) \leqslant \frac{\mathbb{J}_+}{4} + \frac{\varepsilon}{2}. \tag{28}$$

Then if we assume that at $t = 0$, $N_3(0) \gg N_1(0)$ and $N_2(0)$ such that the most energy is stored in the highest frequency mode, from $2N_1 + N_3 \approx N_3(0)$ and $N_1(t) - N_2(t) = N_1(0) - N_2(0)$ we see that $N_3(t)$ decreases and at the same time $N_1(t)$ and $N_2(t)$ increase. So nothing prohibits the energy being completely transferred from the highest frequency mode into the low frequency modes. What we observe is a periodic modulation of the wave amplitudes. We see that most of the initial energy carried by the central frequency mode of the wave, N_3, is transferred to the side bands and the magnitude of the amplitude oscillations is very large. This is the usual Benjamin–Feir instability: the carrier and the two side bands evolve on a periodic cycle of modulation and demodulation known as Fermi–Pasta–Ulam oscillations. In figure 6, we see how the energy exchange is done among the amplitudes N_1, N_2 and N_3 for initial $(N_1, \theta_1) = (\mathbb{I}_+/8, 0)$.

For this initial condition, we have plotted in figure 7 the shape of the wave $\eta(x, t)$. The periodic modulation and demodulation of the three modes give a shape of the wave which is a modulated travelling wave.

- We can also see exchanges of energy for $\mathbb{I}_+ = \mathbb{J}_+/2$, i.e., on the segment $C_+(\mathbb{J}_+/2)$ and for initial conditions so that $N_3(0)$ is close to zero and N_1, N_2 lie on $C_+(\mathbb{J}_+/2)$ so that

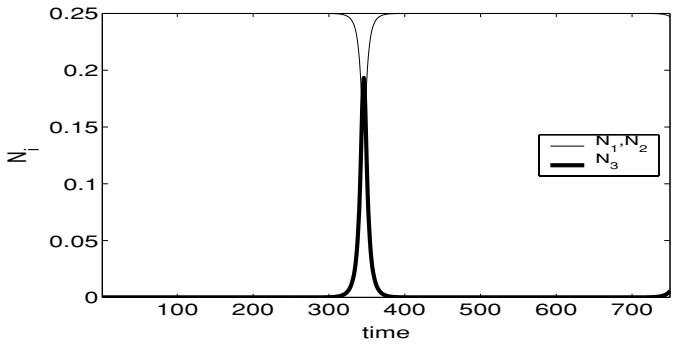

Figure 8. Temporal evolution of modes N_i for $i = 1, 2, 3$, for Hamiltonian (19) with one resonance, $\mathbb{J}_+ = 1$, $\mathbb{I}_+ = \mathbb{J}_+/2$ and an initial condition on the separatrix $(N_1, \theta_1) = (\mathbb{J}_+/4, 2.8)$.

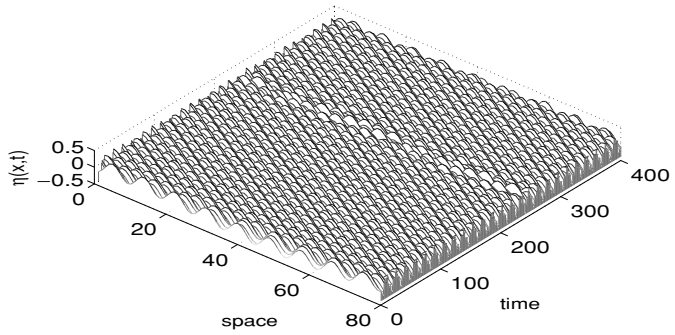

Figure 9. Elevation of the surface $\eta(x, t)$ for Hamiltonian (19) with one resonance for $\mathbb{J}_+ = 1$, $\mathbb{I}_+ = \mathbb{J}_+/2$ and for the fixed point $(N_1, \theta_1) = (\mathbb{J}_+/4, 2.8)$.

$N_1(0) = N_2(0) \approx \mathbb{J}_+/4$. We recall that if $N_1(0) = N_2(0)$ then $N_1(t) = N_2(t)$ and $\mathbb{K}_+ = 0$.

For this case, from equation (9), we conclude that $N_1(t)$ and $N_2(t)$ decrease and $N_3(t)$ grows until it reaches its maximum which is $\mathbb{J}_+/4$. As shown in figure 8, the trajectory stays a long time close to its initial position and then makes a fast excursion before an equally fast return to the departure point. The fast oscillation corresponds to an important exchange of energy between the carrier and the side bands since the carrier almost reaches its maximal energy during the burst. We see in figure 9 the shape of the wave in this case which is quasiperiodic.

4. Dynamics with two resonances

In this section, we analyse the dynamics of Hamiltonian (8) with the two resonances. The phase space is now the product of $\mathbb{E}_+$ by $\mathbb{E}_-$ associated with each resonance. In this case, the dynamics shows a rich variety of regimes allowing a more efficient energy transfer among the modes. We give the dynamics of different orbits in the phase space for different values of the parameters and also give the type of the shape of the wave $\eta(x, t)$.

As in the case of one resonance, we start by simple situations: we explore the dynamics of the points $P_+ \times P_-$, $S_+ \times S_-$, $T_+ \times T_-$ and the segment $(P_+S_+) \times (P_-S_-)$ for which we get the analytical expression of the wave $\eta(x, t)$.

4.1. Dynamics on points $P_+ \times P_-$, $S_+ \times S_-$ and $T_+ \times T_-$

Let us start with the case where the position of the projection of the orbits on $(\mathbb{E}_+) \times (\mathbb{E}_-)$ is fixed at $P_+ \times P_-$ which correspond to $\mathbb{I}_+ = \mathbb{I}_- = 0$ (see figure 1). Since $\mathbb{I}_+ = 2N_1 + N_3$ is a conserved quantity and N_1, N_3 are such that $N_1 \geqslant 0$ and $N_3 \geqslant 0$, we have $N_1 = N_3 = 0$ for all time and $N_2 = \mathbb{J}_+/3$. Similarly, we have $N_{-1} = N_{-3} = 0$ and $N_{-2} = \mathbb{J}_+/3$.

Then for $P_+ \times P_-$, all the actions are constant and the dynamics is connected to the evolution of the angles. The corresponding dynamical equations are

$$\mathrm{i}\frac{\mathrm{d}b_2(t)}{\mathrm{d}t} = (3 + 2U_2(N_2 - 2N_{-2}))b_2, \tag{29}$$

$$\mathrm{i}\frac{\mathrm{d}b_{-2}(t)}{\mathrm{d}t} = (3 + 2U_2(N_{-2} - 2N_2))b_{-2}. \tag{30}$$

The solution in $b_j(t)$ is then

$$b_2(t) = \sqrt{\mathbb{J}_+/3}\exp(-\mathrm{i}(9ct + \phi_+)), \qquad b_{-2}(t) = \sqrt{\mathbb{J}_+/3}\exp(-\mathrm{i}(9\alpha ct + \phi_-)),$$
$$N_j(t) = 0, \qquad \text{for} \quad j = 1, -1, 3, -3, \tag{31}$$

where

$$\alpha = \frac{J_0 + \mathbb{J}_- - 2\mathbb{J}_+}{J_0 + \mathbb{J}_+ - 2\mathbb{J}_-}, \qquad c = \frac{1}{3}\left(1 + \frac{\mathbb{J}_+ - 2\mathbb{J}_-}{J_0}\right) \qquad \text{and} \qquad J_0 = \frac{9}{2U_2}. \tag{32}$$

We note that α is related to $\mathbb{J}_+$ and $\mathbb{J}_-$ by

$$(1 + 2\alpha)\mathbb{J}_- - (\alpha + 2)\mathbb{J}_+ = (\alpha - 1)J_0. \tag{33}$$

The expression of the shape $\eta(x, t)$ is given by

$$\eta(x, t) = \frac{g^{-1/4}}{2\pi\sqrt{2}} \sum_{j=1,2,3} |k_j|^{1/4}((a_j + a_{-j}^*)\,\mathrm{e}^{\mathrm{i}k_j x} + (a_j^* + a_{-j})\,\mathrm{e}^{-\mathrm{i}k_j x}), \tag{34}$$

where the variables a_j, as a function of b_j are given by (see remark 1 at the end of section 2):

$$a_j = b_j + 3\widetilde{V}^{(4)}_{j,j,-j,-j} b_{-j}^{*2} b_j^*, \qquad \text{for} \quad j = 1, 2, 3. \tag{35}$$

Similarly a_{-j} is given by replacing k_j by $-k_j$ in equation (35), and $a_j = 0$ for $j \neq 2$, $j \neq -2$.

Then we deduce the surface shape:

$$\eta(x, t) = \frac{g^{-1/4}}{\pi\sqrt{2}}[\sqrt{\mathbb{J}_+}\cos(9(x - ct) - \phi_+) + \sqrt{\mathbb{J}_-}\cos(9(x + \alpha ct) + \phi_-)$$
$$+ V\mathbb{J}_-\sqrt{\mathbb{J}_+}\cos(9(x + (2\alpha + 1)ct) + 2\phi_- + \phi_+)$$
$$+ V\mathbb{J}_+\sqrt{\mathbb{J}_-}\cos(9(x - (\alpha + 2)ct) - 2\phi_+ - \phi_-)], \tag{36}$$

where $V = \widetilde{V}^{(4)}_{2,2,-2,-2}$.

The wave is the sum of four travelling waves with four *a priori* different velocities c, αc, $(2\alpha + 1)c$ and $(\alpha + 2)c$.

According to the values of $\mathbb{J}_+$ and $\mathbb{J}_-$ and more precisely, depending on α, these solutions are fixed points, travelling or standing waves, periodic or quasiperiodic solutions.

- If $\mathbb{J}_+ = \mathbb{J}_-$, then $\alpha = 1$. We deduce the shape of the wave:

$$\eta(x, t) = \frac{g^{-1/4}\sqrt{2}}{\pi}\sqrt{\mathbb{J}_+}\cos\left(9x - \frac{\phi_+ - \phi_-}{2}\right)$$
$$\times\left(\cos\left(9ct + \frac{\phi_+ + \phi_-}{2}\right) + V\mathbb{J}_+\cos\left(27ct + 3\frac{\phi_+ + \phi_-}{2}\right)\right).$$

  which is a standing wave. Such a wave is represented in figure 10(*a*).

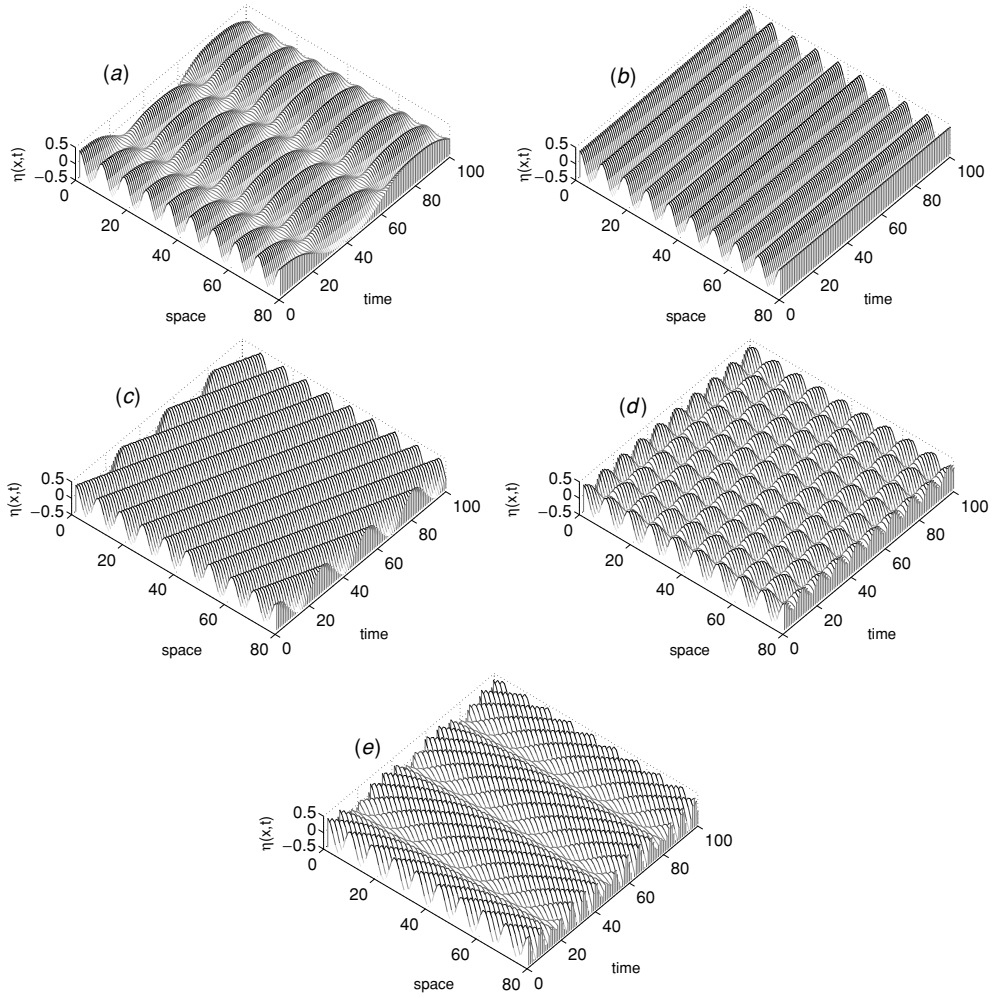

Figure 10. Plots of $\eta(x,t)$ for Hamiltonian (8) with two resonances and for different values of α: (*a*) standing wave $\alpha = 1$, (*b*) stationary wave α indefinite $c = 0$, (*c*) travelling wave $\alpha = -1$, (*d*) time periodic wave $\alpha \in \mathbb{Q}$ $(-\mathbb{J}_+ + 2\mathbb{J}_- = J_0)$, (*e*) time quasiperiodic wave $\alpha = \sqrt{0.4}$.

- For the particular case $\mathbb{J}_+ = \mathbb{J}_- = J_0$, α is not defined and the velocities c and αc vanish. The expression for the surface wave is

$$\eta(x,t) = \frac{g^{-1/4}\sqrt{2}}{\pi}\sqrt{\mathbb{J}_+}\left(\cos\left(9x - \frac{\phi_+ - \phi_-}{2}\right)\right) \times \left(\cos\left(\frac{\phi_+ + \phi_-}{2}\right) + V\mathbb{J}_+\cos\left(3\frac{\phi_+ + \phi_-}{2}\right)\right).$$

  The wave is stationary (see figure 10(*b*)) and its amplitude is a function of the initial phases.

- When $\mathbb{J}_+ + \mathbb{J}_- = 2J_0$ so that $\alpha = -1$, we have a unique family of travelling waves with velocity c whose shape is given by

$$\eta(x,t) = \frac{g^{-1/4}}{\pi\sqrt{2}}[\sqrt{\mathbb{J}_+}\cos(9(x-ct)-\phi_+) + \sqrt{\mathbb{J}_-}\cos(9(x-ct)+\phi_-) + V\mathbb{J}_-\sqrt{\mathbb{J}_+}\cos(9(x-ct)+2\phi_-+\phi_+) + V\mathbb{J}_+\sqrt{\mathbb{J}_-}\cos(9(x-ct)-2\phi_+-\phi_-)]. \quad (37)$$

Figure 10(*c*) shows the elevation of this surface.

- Time periodic waves are obtained for $\alpha \in \mathbb{Q}$ including the particular case $-\mathbb{J}_+ + 2\mathbb{J}_- = J_0$ and $-\mathbb{J}_- + 2\mathbb{J}_+ = J_0$, for which α is respectively indefinite or zero.

  The ratios between the four angles, evolving in time, which are $-ct, \alpha ct, (2\alpha+1)ct$ and $-(\alpha+2)ct$ are rational. The wave is periodic both in space and time, forming the square-shaped patterns as observed in figure 10(*d*).
- In the case where α is irrational, the wave is quasiperiodic in time, expressed as a sum of four travelling waves with different velocities. We have plotted such a wave in figure 10(*e*).

We note that a similar variety of regular surface shapes (standing, stationary, travelling, time-periodic and quasiperiodic waves) are obtained for the two other points of $(\mathbb{E}_+) \times (\mathbb{E}_-)$ which are $S_+ \times S_-$, $T_+ \times T_-$, and for the points $P_+ \times S_-$, $P_+ \times T_-$, $S_+ \times T_-$, $S_+ \times P_-$, $T_+ \times S_-$ and $T_+ \times P_-$.

4.2. Dynamics of a point on the segment $(P_+S_+) \times (P_-S_-)$

We consider the point which is at the intersection of $C_+(\mathbb{I}_+) \times C_-(\mathbb{I}_-)$ and $(P_+S_+) \times (P_-S_-)$. This point is such that $b_3(0) = 0$ and $b_{-3}(0) = 0$. From equations of motion of Hamiltonian (8), we deduce $b_3(t) = 0$ and $b_{-3}(t) = 0$ for any time. From the invariants we obtain that N_1, N_2, N_{-1} and N_{-2} are constant and equal to $N_1(t) = \mathbb{I}_+/2$ and $N_2(t) = (2\mathbb{J}_+ - \mathbb{I}_+)/6$, $N_{-1}(t) = \mathbb{I}_-/2$ and $N_{-2}(t) = (2\mathbb{J}_- - \mathbb{I}_-)/6$. The equations of motion become

$$\frac{\mathrm{d}b_1}{\mathrm{d}t} = -\mathrm{i}\left(1 + \left(U_1 - \frac{V_{21}}{6}\right)\mathbb{I}_+ - \left(2U_1 + \frac{V_{-21}}{6}\right)\mathbb{I}_- + \frac{V_{21}}{3}\mathbb{J}_+ + \frac{V_{-21}}{3}\mathbb{J}_-\right)b_1,$$

$$\frac{\mathrm{d}b_2}{\mathrm{d}t} = -\mathrm{i}\left(3 + \left(-\frac{U_2}{3} + \frac{V_{21}}{2}\right)\mathbb{I}_+ + \left(\frac{2U_2}{3} + \frac{V_{-21}}{2}\right)\mathbb{I}_- + \frac{2}{3}U_2\mathbb{J}_+ - \frac{4}{3}U_2\mathbb{J}_-\right)b_2,$$

$$\frac{\mathrm{d}b_{-1}}{\mathrm{d}t} = -\mathrm{i}\left(1 - \left(2U_1 + \frac{V_{-21}}{6}\right)\mathbb{I}_+ + \left(U_1 - \frac{V_{21}}{6}\right)\mathbb{I}_- + \frac{V_{-21}}{3}\mathbb{J}_+ + \frac{V_{21}}{3}\mathbb{J}_-\right)b_{-1},$$

$$\frac{\mathrm{d}b_{-2}}{\mathrm{d}t} = -\mathrm{i}\left(3 + \left(\frac{2U_2}{3} + \frac{V_{-21}}{2}\right)\mathbb{I}_+ + \left(-\frac{U_2}{3} + \frac{V_{21}}{2}\right)\mathbb{I}_- - \frac{4}{3}U_2\mathbb{J}_+ + \frac{2}{3}U_2\mathbb{J}_-\right)b_{-2}.$$

We deduce the expression for the shape of the wave:

$$\eta(x,t) = \frac{g^{-1/4}}{2\pi}[\sqrt{\mathbb{I}_+}\cos(x + c_1t + \alpha_1) + \sqrt{2\mathbb{J}_+ - \mathbb{I}_+}\cos(9(x - c_2t) + \alpha_2) + \sqrt{\mathbb{I}_-}\cos(x + c_{-1}t + \alpha_{-1}) + \sqrt{2\mathbb{J}_- - \mathbb{I}_-}\cos(9(x - c_{-2}t) + \alpha_{-2})], \quad (38)$$

where

$$c_1 = 1 + (U_1 + V_{21}/6)\mathbb{I}_+ - (2U_1 + V_{-21}/6)\mathbb{I}_- + V_{21}\mathbb{J}_+/3 + V_{-21}\mathbb{J}_-/3,$$

$$c_2 = [3 + (-U_2/3 + V_{21}/2)\mathbb{I}_+ + (2U_2/3 + V_{-21}/2)\mathbb{I}_- + 2U_2\mathbb{J}_+/3 - 4U_2\mathbb{J}_-/3]/9,$$

$$c_{-1} = 1 - (2U_1 + V_{-21}/6)\mathbb{I}_+ + (U_1 + V_{21}/6)\mathbb{I}_- + V_{-21}\mathbb{J}_+/3 + V_{21}\mathbb{J}_-/3$$

and

$$c_{-2} = [3 + (2U_2/3 + V_{-21}/2)\mathbb{I}_+ + (-U_2/3 + V_{21}/2)\mathbb{I}_- - 4U_2\mathbb{J}_+/3 + 2U_2\mathbb{J}_-/3]/9.$$

This wave is the sum of four travelling waves with four different velocities.

4.3. Dynamics of orbits on the segment (P_+S_+) times the interior of $C_-(\mathbb{I}_-)$

We consider the dynamics of (P_+S_+) times the interior of $C_-(\mathbb{I}_-)$ (or similarly the interior of $C_+(\mathbb{I}_+)$ times (P_-S_-)). We have $b_3(t) = 0$ for all t, so $N_3(t) = 0$ is a constant of motion and $N_1(t)$ and $N_2(t)$ are constant for all t. We have now a system with five degrees of freedom b_1, b_2, b_{-1}, b_{-2} and b_{-3} with five constants of motion, $\mathbb{I}_+, \mathbb{I}_-, \mathbb{J}_+, \mathbb{J}_-$ and H. It is then integrable. The modes b_1 and b_2 evolve with a constant modulus and a phase depending on $|b_{-1}|$, $|b_{-2}|$ and $|b_{-3}|$. The dynamics of the modes b_{-1}, b_{-2} and b_{-3} in $C_-(\mathbb{I}_-)$ depend on the second resonance just through the moduli of b_1 and b_2 which are constant. So the exchanges of energy on $C_-(\mathbb{I}_-)$ are not influenced by the evolution of b_1 and b_2. The dynamics of the modes b_{-1}, b_{-2} and b_{-3} is then similar to that studied in the case with one resonance in section 3.

4.4. Dynamics in the interior of $C_+(\mathbb{I}_+) \times C_-(\mathbb{I}_-)$

In order to study the dynamics on the nontrivial sets $C_+(\mathbb{I}_+) \times C_-(\mathbb{I}_-)$ on the interior of the phase space $(\mathbb{E}_+) \times (\mathbb{E}_-)$, i.e., such that N_j are strictly positive for $j = -1, -2, -3, 1, 2, 3$, we perform a canonical transformation in action-angle coordinates, $b_j = \sqrt{N_j}\,\mathrm{e}^{-\mathrm{i}\Phi_j}$, and Hamiltonian (8) becomes

$$\begin{aligned} H = \sum_{j=1,2,3} \omega_j(N_j + N_{-j}) + \sum_{j=1,2,3} U_j\big(N_j^2 + N_{-j}^2 - 4N_jN_{-j}\big) + V_{21}(N_1N_2 + N_{-1}N_{-2}) \\ + V_{-21}(N_1N_{-2} + N_{-1}N_2) - V_{31}(N_1N_3 + N_{-1}N_{-3}) + V_{-31}(N_1N_{-3} + N_{-1}N_3) \\ + V_{23}(N_2N_3 + N_{-2}N_{-3}) - V_{-23}(N_2N_{-3} + N_{-2}N_3) \\ + W\sqrt{N_1N_2}N_3\cos(\Phi_1 + \Phi_2 - 2\Phi_3) \\ + W\sqrt{N_{-1}N_{-2}}N_{-3}\cos(\Phi_{-1} + \Phi_{-2} - 2\Phi_{-3}). \end{aligned} \tag{39}$$

Using the invariants $\mathbb{I}_+, \mathbb{I}_-, \mathbb{J}_+$ and $\mathbb{J}_-$, we now proceed to the reduction of the dimension of the system to two degrees of freedom.

We perform as in the case with one resonance the canonical transformation from $(N_1, N_2, N_3, N_{-1}, N_{-2}, N_{-3}, \Phi_1, \Phi_2, \Phi_3, \Phi_{-1}, \Phi_{-2}, \Phi_{-3})$ to $(\tilde{N}_1, \mathbb{K}_+, \mathbb{I}_+, \tilde{N}_{-1}, \mathbb{K}_-, \mathbb{I}_-, \theta_1, \theta_2, \theta_3, \theta_{-1}, \theta_{-2}, \theta_{-3})$:

$$\begin{aligned} &\tilde{N}_1 = N_1, && \mathbb{K}_+ = N_1 - N_2, && \mathbb{I}_+ = 2N_1 + N_3, \\ &\theta_1 = \Phi_1 + \Phi_2 - 2\Phi_3, && \theta_2 = -\Phi_2, && \theta_3 = \Phi_3, \\ &\tilde{N}_{-1} = N_{-1}, && \mathbb{K}_- = N_{-1} - N_{-2}, && \mathbb{I}_- = 2N_{-1} + N_{-3}, \\ &\theta_{-1} = \Phi_{-1} + \Phi_{-2} - 2\Phi_{-3}, && \theta_{-2} = -\Phi_{-2}, && \theta_{-3} = \Phi_{-3}. \end{aligned} \tag{40}$$

The actions $\tilde{N}_1, \mathbb{K}_+, \mathbb{I}_+, \tilde{N}_{-1}, \mathbb{K}_-$ and $\mathbb{I}_-$ are now, respectively, conjugate to angles $\theta_1, \theta_2, \theta_3, \theta_{-1}, \theta_{-2}$ and θ_{-3}. In what follows, we use N_1, N_{-1} instead of $\tilde{N}_1$ and $\tilde{N}_{-1}$ for simplicity. Hamiltonian (39) becomes

$$\begin{aligned} H = \Omega_0 + \Omega_1N_1 + \Omega_{-1}N_{-1} + \Omega_2\big(N_1^2 + N_{-1}^2\big) + \Omega_3N_1N_{-1} \\ + W\sqrt{N_1}\sqrt{N_1 - \mathbb{K}_+}(\mathbb{I}_+ - 2N_1)\cos\theta_1 \\ + W\sqrt{N_{-1}}\sqrt{N_{-1} - \mathbb{K}_-}(\mathbb{I}_- - 2N_{-1})\cos\theta_{-1}, \end{aligned} \tag{41}$$

where the functions Ω_0, Ω_1 and Ω_{-1} only depend on the actions $\mathbb{I}_+, \mathbb{K}_+, \mathbb{I}_-, \mathbb{K}_-$ and Ω_2 and Ω_3 are constant:

$$\begin{aligned} \Omega_0 = -3(\mathbb{K}_- + \mathbb{K}_+) + 2(\mathbb{I}_- + \mathbb{I}_+) + U_3\big(\mathbb{I}_-^2 + \mathbb{I}_+^2 - 4\mathbb{I}_+\mathbb{I}_-\big) + U_2\big(\mathbb{K}_-^2 + \mathbb{K}_+^2 - 4\mathbb{K}_+\mathbb{K}_-\big) \\ - V_{23}(\mathbb{I}_+\mathbb{K}_+ + \mathbb{I}_-\mathbb{K}_-) + V_{-23}(\mathbb{I}_+\mathbb{K}_- + \mathbb{I}_-\mathbb{K}_+), \end{aligned}$$

$$\begin{aligned}
\Omega_1 &= 2U_2(-\mathbb{K}_+ + 2\mathbb{K}_-) + 4U_3(-\mathbb{I}_+ + 2\mathbb{I}_-) - V_{21}\mathbb{K}_+ - V_{-21}\mathbb{K}_- \\
&\quad - V_{31}\mathbb{I}_+ + V_{-31}\mathbb{I}_- + V_{23}(\mathbb{I}_+ + 2\mathbb{K}_+) - V_{-23}(\mathbb{I}_- + 2\mathbb{K}_-), \\
\Omega_{-1} &= 2U_2(-\mathbb{K}_- + 2\mathbb{K}_+) + 4U_3(-\mathbb{I}_- + 2\mathbb{I}_+) - V_{21}\mathbb{K}_- - V_{-21}\mathbb{K}_+ \\
&\quad - V_{31}\mathbb{I}_- + V_{-31}\mathbb{I}_+ + V_{23}(\mathbb{I}_- + 2\mathbb{K}_-) - V_{-23}(\mathbb{I}_+ + 2\mathbb{K}_+), \\
\Omega_2 &= U_1 + U_2 + 4U_3 + V_{21} + 2V_{31} - 2V_{23}, \\
\Omega_3 &= -4U_1 - 4U_2 - 16U_3 + 2V_{-21} - 4V_{-31} + 4V_{-23}.
\end{aligned} \tag{42}$$

Since Hamiltonian (41) does not depend on $\theta_2, \theta_3, \theta_{-2}$ and θ_{-3}, we can consider $\mathbb{I}_+, \mathbb{K}_+, \mathbb{I}_-, \mathbb{K}_-$ as parameters of the system for the dynamics of N_1, N_{-1}, θ_1 and θ_{-1}.

We recall that N_1 and N_{-1} are such that $\max(0, \mathbb{K}_+) < N_1 < \mathbb{I}_+/2$ and $\max(0, \mathbb{K}_-) < N_{-1} < \mathbb{I}_-/2$. The accessible part of phase space is thus contained into the product of two interiors of a circle or an annulus, depending on the values of $\mathbb{I}_+$ and $\mathbb{I}_-$.

In order to visualize the dynamics on $C_+(\mathbb{I}_+) \times C_-(\mathbb{I}_-)$, we compute Poincaré sections of the dynamics and then we project these surfaces on the (N_1, θ_1)-plane. The Poincaré sections Σ are constructed in the following way:

$$\Sigma = \left\{ (N_1, N_{-1}, \theta_1, \theta_{-1}) : \theta_{-1} = 0, \frac{\mathrm{d}\theta_{-1}}{\mathrm{d}t} < 0, H = H(N_1, N_{-1}, \theta_1, \theta_{-1}, \mathbb{I}_+, \mathbb{I}_-) \right\}. \tag{43}$$

Now the parameters are the energy H, and the four invariants $\mathbb{I}_+, \mathbb{I}_-, \mathbb{J}_+$ and $\mathbb{J}_-$.

Since Hamiltonian (39) has two degrees of freedom, Poincaré sections are two dimensional and therefore we get an accurate picture of the dynamics by looking at the projections of Σ on (N_1, θ_1). For most of the values of the parameters, these sections show a rich variety for the dynamics, a mixed phase space with regular and chaotic behaviour.

We give a plot of some projections for $\mathbb{J}_+ = \mathbb{J}_- = 1$, $H = 2$ and for different values of $\mathbb{I}_+ = \mathbb{I}_-$: from $\mathbb{I}_+ = \mathbb{I}_- = 0.3$ to $\mathbb{I}_+ = \mathbb{I}_- = 0.8$.

We observe in figure 11(*a*), when $\mathbb{I}_+$ and $\mathbb{I}_-$ are near zero so that we are in the neighbourhood of the point $P_+ \times P_-$, the motion is completely regular and all the orbits lie on invariant tori. For this value of H, the dynamics occurs close to the centre of the accessible region of phase space. The elliptic and hyperbolic fixed points of the Poincaré sections are of the same type as those of the elliptic and hyperbolic orbits of the case with one resonance. Besides these points, there are one elliptic and two hyperbolic points due to the second resonance. We recall that the invariants depend on the variables of only one resonance. So, for small values of $\mathbb{I}_+$ and $\mathbb{I}_-$, we can make the same reasoning as for the one resonance case and we can conclude that in the neighbourhood of the point $P_+ \times P_-$, the exchanges of energy between the modes are not significant and it leads to regular behaviour of the system. Thus, in the system with small values of $\mathbb{I}_+$ and $\mathbb{I}_-$, the only possible motion for the system is periodic or quasiperiodic in time, corresponding to regular shapes for the wave $\eta(x, t)$ (see section 3).

To undergo a transition to chaos, we increase the parameter $\mathbb{I}_+$ (which increases the effect of the nonlinear terms up to a certain threshold), and for a value of $\mathbb{I}_+$ in the neighbourhood of $\mathbb{I}_+ = \mathbb{J}_+/2$, we see in figures 11(*b*) and (*c*) that the phase space is made up of regular and chaotic motion. Chaotic trajectories are located between regular trajectories (on invariant tori). We observe that the motion is clearly affected by the vicinity of hyperbolic points: the irregular motion appears in the neighbourhood of hyperbolic periodic orbits breaking up their neighbouring KAM tori.

The first of the two regular zones which surround the chaotic sea (outer region) is obtained for large amplitudes of the modes of low frequency N_1 and N_{-1} which are larger than the ones of high frequency modes N_3 and N_{-3}. The second regular zone (inner region) is obtained when

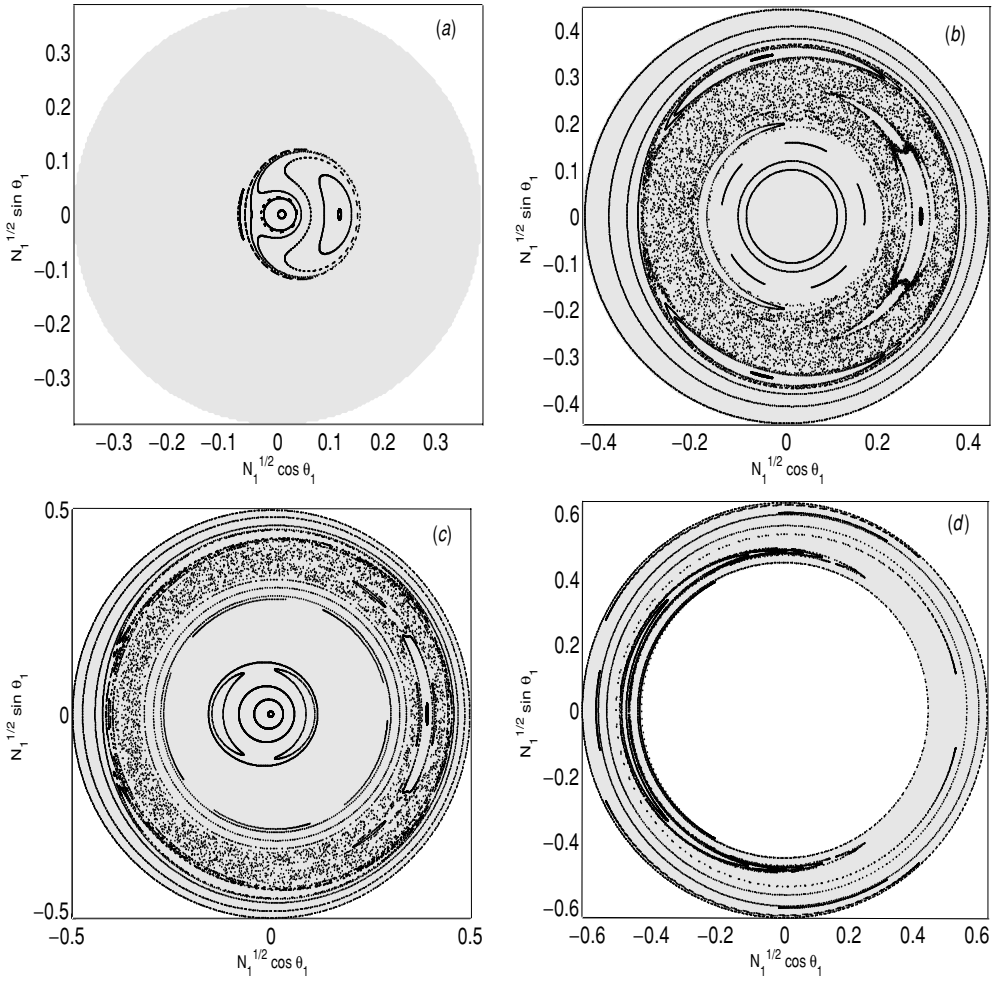

Figure 11. Poincaré sections for Hamiltonian (39) with two resonances for $H = 2$, $\mathbb{J}_+ = \mathbb{J}_- = 1$ and for different values of $\mathbb{I}_+$: (*a*) $\mathbb{I}_+ = \mathbb{I}_- = 0.3$, (*b*) $\mathbb{I}_+ = \mathbb{I}_- = 0.4$, (*c*) $\mathbb{I}_+ = \mathbb{I}_- = 0.5$, (*d*) $\mathbb{I}_+ = \mathbb{I}_- = 0.8$. The grey region is the accessible region where $\max(0, \mathbb{K}_+) \leqslant N_1 \leqslant \mathbb{I}_+/2$.

the amplitude of the modes of low frequency N_1 and N_{-1} are small. In these regular zones, the exchanges of energy are not significant and give rise to regular behaviour of the system. On the other hand, for orbits close to the hyperbolic points, the modes oscillate chaotically (see figure 12). As the parameter $\mathbb{I}_+$ increases, the region in which N_1 evolves shrinks and all the orbits become stable, the system admits only regular behaviour as can be seen in figure 11(*d*). This is due to the fact that, in the accessible region, the values of N_1 are larger than those of N_3 and for this case the exchanges among the modes are not significant.

We conclude that chaotic exchanges of energy may be done in the neighbourhood of $C_+\left(\frac{\mathbb{J}_+}{2}\right) \times C_-\left(\frac{\mathbb{J}_-}{2}\right)$. In figure 12, we give the plot of the modes $N_j(t)$, $j = 1, 2, 3, -1, -2, -3$; and in figure 13, we give the shape of the wave $\eta(x, t)$ for $\mathbb{I}_+ = \mathbb{I}_- = \mathbb{J}_+/2$ and for an initial condition $(N_1, \theta_1) = (0.152, -3.07)$ which is in the chaotic region. In these two plots, we see the irregular motion of the modes N_j (chaotic exchanges of energy) and the chaotic structure of $\eta(x, t)$. We note that in the chaotic zones, significant energy exchanges occur among the modes.

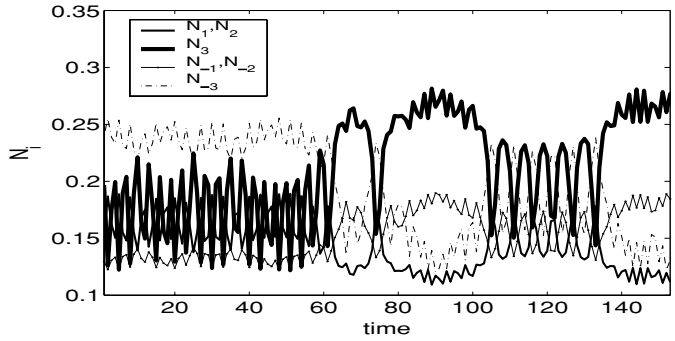

Figure 12. Time evolution of N_j for $j = -1, -2, -3, 1, 2, 3$, for Hamiltonian (39) with two resonances and for $\mathbb{I}_+ = \mathbb{I}_- = 0.5$ and for an initial condition in the chaotic region $(N_1, \theta_1) = (0.152, -3.07)$.

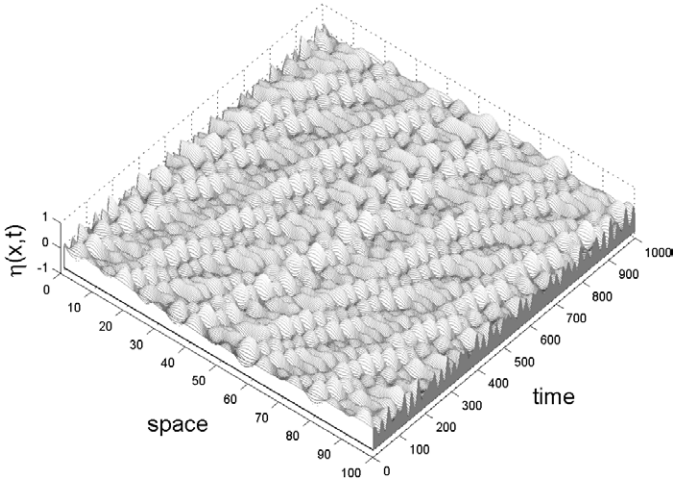

Figure 13. Shape of the wave $\eta(x, t)$ for $\mathbb{I}_+ = \mathbb{I}_- = 0.5$ for Hamiltonian (39) with two resonances and for an initial condition in the chaotic region $(N_1, \theta_1) = (0.152, -3.07)$.

5. Conclusion

Following the framework of Zakharov in [3] and Krazitskii in [18], we have built a Hamiltonian model for six interacting waves for gravity water waves in infinite depth. The interactions are those of two coupled Benjamin–Feir resonances. The knowledge of four constants of motion allowed us to reduce the system to a Hamiltonian system with two degrees of freedom. We have first studied the dynamical properties of the Hamiltonian with only one resonance which is integrable. This simple case allowed us to understand the basics of the full dynamics. A whole variety of solutions have been found in this simple case such as travelling, time periodic and quasiperiodic waves. We showed that exchanges of energy occur in the zone of phase space where the energies initially put into the two side bands are equally important and when the energy in the central mode is the same as the sum of the energies of the two side bands. This situation corresponds to phase space regions close to the separatrices. All these exchanges are done in a periodic way. Thus, when we take into account only one resonance, the only possible motion is a regular time quasiperiodic (and space periodic) wave.

Then we have studied the dynamics with two resonances. Besides the regular waves such as travelling, time periodic and quasiperiodic waves, the full system exhibits stationary and standing waves. We have visualized the dynamics using numerical Poincaré sections. We have shown that the system with two coupled resonances undergoes a transition to chaos. Chaotic behaviour occurs in the regions where the energies of the side bands of each resonance are equally important and near the broken separatrices. In this case, there is a strong exchange of energy between all the modes and it is done in a chaotic way.

References

[1] Benjamin T B and Feir J E 1967 The disintegration of wave trains in deep water: part 1. Theory *J. Fluid Mech.* **27** 417

[2] Lighthill M J 1967 Some special cases treated by Whitham theory *Proc. R. Soc. Lond.* A **299** 28

[3] Zakharov V E 1968 Stability of periodic waves of finite amplitude on the surface of a deep fluid *J. Appl. Mech. Tech. Phys. (USSR)* **51** 269

[4] Lake B M, Yuen H C, Rungaldier H and Ferguson W E 1977 Nonlinear deep-water waves: theory and experiment: part 2. Evolution of a continuous wave train *J. Fluid Mech.* **83** 49

[5] Fermi E, Pasta J and Ulam S 1955 Studies of nonlinear problems *Collected Papers of Enrico Fermi* **2** (Chicago, IL: University of Chicago Press) p 978

[6] Craig W 1996 Birkhoff normal forms for water waves *Contemp. Math.* **200** 57

[7] Craig W and Groves M D 1994 Hamiltonian long-wave approximations to the water-wave problem *Wave Motion* **19** 367

[8] Dias F and Kharif C 1999 Nonlinear gravity and capillary-gravity waves *Ann. Rev. Fluid Mech.* **31** 301

[9] Shemer L and Stiassnie M 1985 *Initial Instability and Long-Time Evolution of Stokes Waves in the Ocean Surface: Wave Breaking, Turbulent Mixing and Radio Probing* ed Y Toba and H Mitsuyasu (Dordrecht: Reidel)

[10] Stiasnie M and Shemer L 1987 Energy computations for evolution of class I and II instabilities of Stokes waves *J. Fluid. Mech.* **174** 299

[11] Shrira V I, Badulin S I and Kharif C 1996 A model of water wave horse-shoe patterns *J. Fluid Mech.* **318** 375

[12] Badulin S I, Shrira V I, Kharif C and Ioualalen M 1995 On two approaches to the problem of instability of short-crested water waves *J. Fluid Mech.* **303** 272

[13] Benzekri T, Lima R and Vittot M 2000 Non-permanent form solutions in the Hamiltonian formulation of surface water waves *Eur. J. Mech.* B **19** 379

[14] Caponi E A, Saffman P G and Yuen H C 1982 Instability and confined chaos in nonlinear dispersive wave system *Phys. Fluids* **25** 2159

[15] Zufiria J A 1988 Oscillatory spatial periodic weakly nonlinear gravity waves on deep water *J. Fluid Mech.* **191** 341

[16] Craig W and Groves M D 2000 Normal forms for wave motion in fluid interfaces *Wave Motion* **31** 21

[17] Dias F and Bridges T J 1994 Geometric aspects of spatially periodic interfacial waves *Stud. Appl. Math.* **93** 93

[18] Krasitskii V P 1994 On reduced equations in the Hamiltonian theory of weakly nonlinear surface waves *J. Fluid Mech.* **272** 1

[19] Dyachenko A I and Zakharov V E 1994 Is free surface hydrodynamics an integrable system? *Phys. Lett.* A **190** 144

[20] Craig W and Worfolk P 1995 An integrable normal form for water waves in infinite depth *Physica* D **84** 513

[21] Trulsen K, Kliakhandler I, Dysthe K B and Velarde M G 2000 On weakly nonlinear modulation of waves on deep water *Phys. Fluids* **12** 2432